Available online at www.sciencedirect.com
ScienceDirect
International Journal of Heat and Mass Transfer 51 (2008) 1962–1969
International Journal of HEAT and MASS TRANSFER
www.elsevier.com/locate/ijhmt

Influence of fuel fraction gradient on triple flame velocity in plain and axis-symmetrical channels

K.V. Dobrego [a], I.M. Kozlov [a], V.V. Vasiliev [a,*], J.-P. Martin [b], P. Gillon [b]

[a] Heat and Mass Transfer Institute, National Academy of Sciences of Belarus P. Brovki Street 15, Minsk 220072, Belarus
[b] LCSR, Lab. Aerothermique CNRS 1C, Avenue de la Recherche Scientifique, 45071 Orleans Cedex 2, France

Received 2 March 2007
Available online 22 October 2007

Abstract

Dynamics of laminar triple flame investigated numerically for the different mixture degrees. One-step methane–air chemistry adequate to reach and lean mixture combustion was accepted. Velocity of triple flame is determined as a function of methane concentration logarithm gradients $\mu = \mathrm{d}(\ln Y_1)/\mathrm{d}x$ (characterizing mixing degree). It is found that maximum velocity of the triple flames correspond to the value of the methane concentration logarithm gradients $\mu \approx 1000\ \mathrm{m}^{-1}$ for plain and $\mu \approx 2000\ \mathrm{m}^{-1}$ for axis-symmetrical channels. The maximum velocity of triple flame in plain and axis-symmetrical channels in the case of non-gradient incoming gas flow is about twice bigger than normal laminar flame velocity $S_\mathrm{f} \approx 2.1 S_\mathrm{l}$.

Keywords: Non-premixed combustion; Triple flame; Flame stabilization

1. Introduction

Combustion of partially premixed or non-premixed fuels is widely spread in burners, engines, turbines and other technological devices. The leading edge of the non-premixed flames has two-dimensional structure where three branches of heat release can be distinguished, two of them spread to reach and lean areas and third – along the stoichiometric line. Existence of triple structure of heat release was first pointed out in the Philips work [1] where flame propagation along the interface between a layer of methane and air has been investigated experimentally. In later investigations it was called tribrachial. Estimation of the tribrachial flame (TF) propagation velocity as function of different parameters of the system is principal and practically important problem. The intrinsic TF velocity defines parameters of flame liftoff and blowout in the torch burners, burning velocity of partially premixed fuel in the combustion chambers. It is also necessary for combustion safety analysis.

Various factors affect the TF speed, including flame stretch, preferential diffusion, heat losses [2] etc., nevertheless the dominant factor is fuel concentration gradient or the mixture fraction gradient in front of flame edge [3]. The mixture fraction gradient determines the thickness of flammable region and thereby the hydrodynamics of ambient flow. Principally, the TF velocity increases relatively to normal stoichiometric flame speed S_l due to flow lines redirection before the flame and decreases due to flame front stretch and energy loss [4,5]. These two trends determine the nonmonotonous character of velocity dependence on mixture fraction gradient.

Dold [6] and Hartley and Dold [7] studied the effect of mixture fraction gradients in the region of the triple point by assuming activation energy asymptotics, small concentration gradient in upstream direction (the last omitted in [7]) and by neglecting the gas thermal expansion. For a moderately curved flame the velocity is determined as solution of an integral equation.

* Corresponding author. Tel.: +375 (17) 2842217.
E-mail address: vvv@dnp.itmo.by (V.V. Vasiliev).

0017-9310/$ - see front matter © 2007 Elsevier Ltd. All rights reserved.
doi:10.1016/j.ijheatmasstransfer.2007.06.004

Nomenclature

D	diffusion coefficient
d	width of the channel and simulation domain
d_{sat}	characteristic width of channel when influence of the walls is negligible
E	activation energy
H	gas enthalpy
h_i	specific enthalpy of ith gaseous component
L	length of the channel and simulation domain
l_f	flame front width
M	mean molecular mass
M_i	molecular mass of ith gaseous component
N_r	normalization parameter for reaction rate
$\mathbf{n}$	normal vector
p_0	gas pressure
p_n	normalization parameter for reaction rate
r	radial coordinate
r_m	radial coordinate of concentration boundary
S_0	flame velocity in the laboratory system of coordinates
S_f	flame speed
S_l	normal laminar stoichiometric flame speed
S_{loc}	local flame speed
R	universal gas constant
$\mathbf{R}$	reference point.
T	temperature
t	time
u	gas velocity
X_i	molar concentration of ith component
x	transverse coordinate
x_m	coordinate of concentration boundary
Δx	spatial mesh step
Y_i	mass concentration of ith component
y	longitude coordinate
y_{max}	coordinate of first local maximum of χ
Δy	space interval for S_0 evaluation
z	reaction rate preexponent factor

Greek symbols

β	Zel'dovich number, $\beta = E(T_{ad} - T_0)/T_{ad}^2$
χ	dimensionless mixing degree
χ_{max}	local maximum of χ
φ	fuel–air equivalence ratio
λ	coefficient of heat conductivity
μ	relative fuel concentration gradient
ν	coefficient of dynamic viscosity
ρ	gas density
$\boldsymbol{\sigma}'$	viscous tensions tensor

Superscript

n	time layer number

Subscripts

0	input or entrance to system
1	fuel
2	oxidizer
ad	adiabatic
b	burned
f	flame or front of the flame
R	value at reference point
st	stoichiometry
u	unburned

Ruetsch et al. [8] studied the effect of heat release on flame speed. They showed that heat release play decisive role in TF propagation. Due to flow redirection the axial velocity along the stoichiometric line reaches a minimum in front of the flame edge. This minimum velocity was found to be close to the stoicheometric laminar burning velocity. Expression $\frac{S_f}{S_l} \propto \sqrt{\frac{\rho_u}{\rho_{b,st}}}$ for the TF asymptotic propagation speed S_f can be derived based on conservation relations [8]. According to the formula S_f can be considerably larger than normal laminar velocity (for $\rho_u/\rho_b = 7$, $S_f/S_l \approx 2.6$). This velocity increase was observed experimentally by Lee and Chung [9].

Direct numerical simulation with detailed chemical reactions mechanisms [10–12] demonstrated that S_f growth is mainly due to the flow redirection effect and the contributions of the differential diffusion and strain were quite small. In the DNS investigations of methanol–air [10] and hydrogen–air [11] non-premixed flames it was also demonstrated that Luis number effect on the flame velocity is negligibly small.

The up to date state of the TF dynamic investigations are presented in Chung's overview [3]. Thus considerable progress in TF physical understanding description was achieved in the recent years. Nevertheless a set of problems are left for further investigation among which is the quantitative characteristics of flow divergence, although the distance of the flow redirection and other parameters of the flow field are utilized for qualitative analysis [5,13]. Direct numerical simulation of practical combustion devices is too complicated task for modern computers. However sufficiently detailed numerical simulation can shed light on most theoretical and practical aspects of TF.

In this work methane–air triple flame velocity is determined numerically as a function of mixture fraction gradient or premixing degree. The results illustrate gas dynamics of triple flames and may be utilized for study of flames lift-off and blowout.

2. Problem statement

Consider diffusion flame propagating in constant velocity flow of partially premixed methane and air, Fig. 1. Methane and air flow rates are in stoicheometric propor-

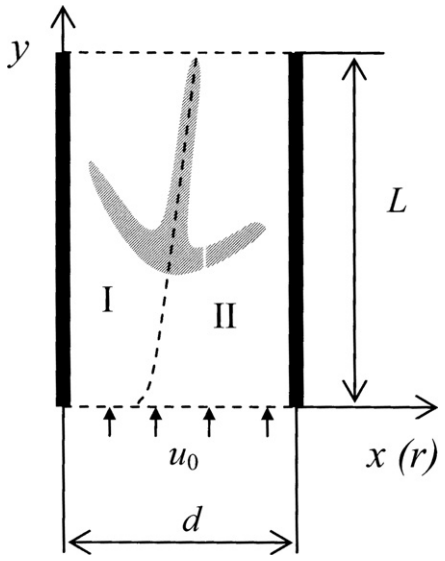

Fig. 1. Scheme of simulated system (plain and axis-symmetrical). Dashed line – stoicheometric line, grey – TF heat release zone. I – fuel rich area, II – fuel lean area.

tion. Flame propagation velocity relative to incoming gas (effective velocity) will be the function of mixing degree and geometry of the system. Evidently in the limiting case of premixed combustible and non-perturbed flow flame velocity is equal to normal laminar flame velocity S_l. Simulated systems are plain channel with width d and length L and axis-symmetrical system of diameter d. Adiabatic walls condition was used for simulations. Gas velocity at the entrance cross-section ($y = 0$) is constant. Hydrodynamic slip condition at the walls was applied.

Thus the described model system is characterized by variable geometry parameters of the combustion chamber and mixture fraction gradient in vicinity of the flame edge. Other parameters – reaction rate constants, diffusivity, conductivity etc. are fixed.

For unique and physically adequate definition of the concentration field at the entrance cross-section the following method was used. One-dimensional diffusion problem was solved with initial conditions:

$$\begin{cases} Y_1 = 1; \quad Y_2 = 0, \quad 0 \leqslant x < x_m, \\ Y_1 = 0; \quad Y_2 = 1, \quad x_m \leqslant x \leqslant d. \end{cases}$$

Here coordinates of boundary x_m (r_m for axis-symmetrical channel) are defined by width (or radius) of the system and stoicheometric ratio φ_{st}.

$$\frac{x_m}{d - x_m} = \varphi_{st} - \text{for plain symmetry channel},$$

$$\frac{4r_m^2}{d^2 - 4r_m^2} = \varphi_{st} - \text{for axis-symmetrical channel}.$$

Both 1-D mixing and following 2-D combustion problem were solved by the same 2DBurner software.

Two parameters were used to characterize mixing degree: dimensionless premixing degree χ and gradient of concentration logarithm μ [4]. The first is defined as follows:

$$\chi = \frac{\frac{1}{d}\int_0^d \rho\sqrt{Y_1(x)Y_2(x)}\,\mathrm{d}x}{\sqrt{(\rho Y_1)_{\max}(\rho Y_2)_{\max}}},$$

where $Y_1(x)$, $Y_2(x)$ – local mass fractions of fuel and oxidizer. The second is:

$$\mu = \frac{1}{Y_1}\frac{\mathrm{d}Y_1}{\mathrm{d}x},$$

where Y_1 – fuel mass concentration. For the channel with $d = 3.2$ mm width relationship between parameters χ and μ is presented on the Fig. 2.

Distribution of the main components fractions corresponding to $\chi = 0.1$ and channel width $d = 3.2$ mm is presented on the Fig. 3.

To determine effective combustion velocity and other parameters of TF we looked for stationary solution for TF. As far as in general case flame is unsteady we accepted the following procedure of obtaining the stable steady-state solution. The coordinate of the flame stabilization y_f was fixed (in most calculations $y_f = 1.6$ mm). At each time step y coordinate of front was determined. Then gas velocity at the entrance u_0^n was changed to u_0^{n+1} to satisfy stabilization

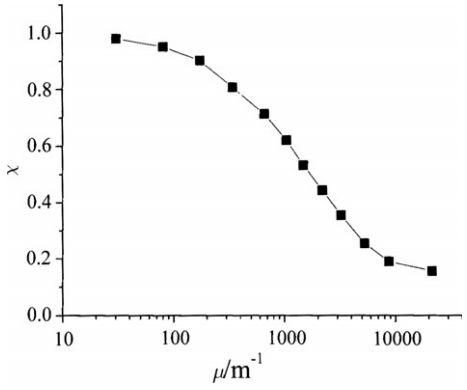

Fig. 2. Correlation between mixing characteristics χ and μ ($d = 3.2$ mm).

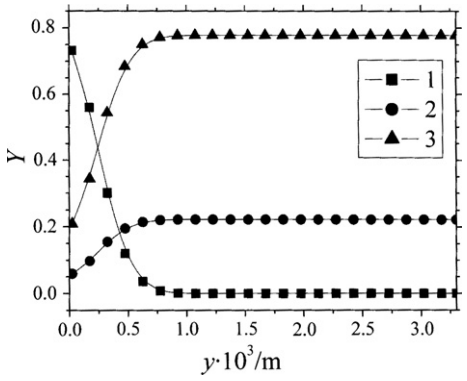

Fig. 3. Distribution of the main components at $y = 0$ cross-section. $\chi_0 = 0.1$ ($d = 3.2$ mm).

of the front at fixed y_f position according to the following formulas:

$$S_0 = \frac{1}{\rho_{y_f-\Delta y} - \rho_{y_f+\Delta y}} \int_{y_f-\Delta y}^{y_f+\Delta y} \frac{\partial \rho}{\partial t}\, dy,$$

$$u_0^{n+1} = \begin{cases} 0, & u_0^n - S_0 < 0, \\ u_0 - S_0, & u_0^n - S_0 \geqslant 0. \end{cases}$$

Combustion front position was defined by maximum heat release.

3. Governing equations

Mathematical model included non-steady equations of continuity, Navier-Stokes, mass conservation for gas components and energy conservation:

$$\frac{d\rho}{dt} = -\rho \nabla \mathbf{u}, \tag{1}$$

$$\rho \frac{d\mathbf{u}}{dt} = -\nabla p + \nabla \boldsymbol{\sigma}', \tag{2}$$

$$\rho \frac{dY_i}{dt} = \dot{\rho}_i + \nabla \cdot (\rho D \nabla Y_i), \quad i = \overline{1,N}, \tag{3}$$

here $\dot{\rho}_i$ – ith component mass generating rate due to chemical reaction (5), $\sum_i \dot{\rho}_i = 0$; D – diffusion coefficient, $\boldsymbol{\sigma}'$ – viscous tensions tenser with components: $(\boldsymbol{\sigma}')_{ik} = \nu\left(\frac{\partial u_i}{\partial x_k} + \frac{\partial u_k}{\partial x_k} - \frac{2}{3}\delta_{ik}\frac{\partial u_i}{\partial x_k}\right)$. Energy conservation equation is written in form of enthalpy conservation with regard to diffusion and heat conductivity processes:

$$\rho \frac{dH}{dt} = \nabla \cdot \left(\rho \sum_i h_i D \nabla Y_i + \lambda \nabla T\right), \tag{4}$$

where h_i – mass enthalpy of ith gaseous component, λ – heat conductivity coefficient. Speed of sound is assumed to be infinitely high.

State of gas in arbitrary point is defined by pressure p_0, temperature T, gas velocity $\mathbf{u}$, gas components mass fractions Y_i together with gas state equations $\rho = \frac{p_0 M}{RT}$ and $H(T, Y_1, \ldots, Y_N) = \sum_t^N Y_i h_i(T)$, where $h_i(T)$ is expressed via polynomials according to CHEMKIN thermodynamics database [14] $\frac{M_i h_i}{RT} = \sum_{j=1}^5 \frac{a_{ij}}{j} T^{j-1} + \frac{a_{6i}}{T}$. Mean molar mass of the gas M is expressed via component concentrations and mass $\frac{1}{M} = \sum_i \frac{Y_i}{M_i}$.

As far as velocity field is determined by pressure field (according to simulation method) boundary conditions applied to the pressure filed as follows. Impermeability and slip condition at the tube's walls:

$$\begin{cases} (\mathbf{n} \cdot \nabla) p = 0, \\ \partial v_z / \partial r|_{\text{wall}} = 0, \\ v_r|_{x=0} = 0, \end{cases}$$

constant pressure condition at the open end cross-section:

$p = p_0$ at $(y = L)$.

Impermeability of walls to gas components

$(\mathbf{n} \cdot \nabla) Y_i = 0,$

adiabatic boundaries conditions

$$\lambda \left.\frac{\partial T}{\partial T}\right|_{\text{wall}} = 0.$$

Reasonably simplified models of diffusion, heat conductivity and viscosity were used. The following approximations with characteristics accuracy 5% in all temperature range were utilized: $\lambda = 1.4 \times 10^{-2} + 4.8 \times 10^{-5} T$, $\frac{\text{W}}{\text{m·K}}$; $v = 4.4 \times 10^{-7} T^{0.65}$, $\frac{\text{kg}}{\text{m·s}}$; $D = 1.13 \times 10^{-4} \frac{T^{1.7}}{p_0}$, $\frac{\text{m}^2}{\text{s}}$.

One-step chemical kinetics was used to simulate methane combustion:

$$CH_4 + 2O_2 \rightarrow CO_2 + 2H_2O. \tag{5}$$

The reaction rate was fitted to satisfy experimental data on normal flame velocity for lean, stoichiometric and rich mixtures and had the following form:

$$\frac{dX_1}{dt} = -\frac{X_1 X_2^{p_n}}{(X_1 + X_2)^{N_r}} z \exp(-E/T), \tag{6}$$

where X_1, X_2 – molar fractions of methane and oxygen correspondingly, p_n and N_r – fixed parameters, z – preexponent factor, $E = 15{,}640$ K – activation energy. Normal flame velocity as a function of the equivalence ratio φ calculated by the model (5), (6) for $p_n = 2$, $N_T = 2$, $z = 7.74 \times 10^8\ \text{s}^{-1}$ together with experimental data [15–19] is presented on the Fig. 4. One can see that the kinetics model describes satisfactorily minor shift of the $S_l(\varphi)$ maximum to the reach mixture area and general shape of the $S_l(\varphi)$ curve.

Adiabatic combustion temperature for stothiometric methane–air mixture was $T_{ad} = 2256$ K, normal laminar flame velocity was $S_l = 0.406$ m/s for this chemical kinetics model. Flame front width l_f, calculated by formula $(\lambda/c\rho)/S_l$ at the temperature of the chemical heat release ignition was $l_f = 0.3$ mm. This value was used as characteristic length scale of the problem.

2DBurner software application package was used for simulation [20]. Analogue of the MAC method generalized for calculating of a compressible gas slow flow taking into consideration thermal conductivity, mass diffusion and viscosity force was used for prediction of the gas motion. A

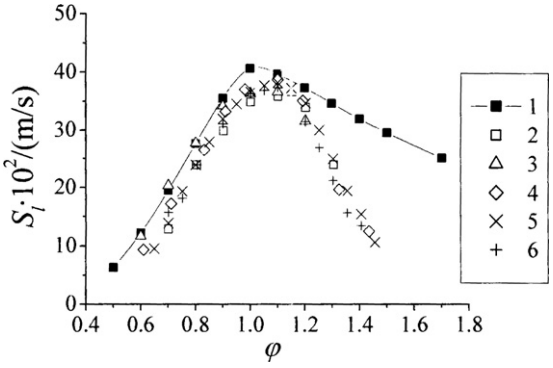

Fig. 4. Normal laminar flame velocity as a function of equivalence ratio. 1 – calculation by the model (5), (6); experimental data: 2 – Hassan et al. [15], 3 – Gu et al. [16], 4 – Vagelopoulos et al. [17], 5 – Van Maaren et al. [18] and 6 – Vagelopoulos and Egolfopoulos [19].

similar method for gas free convection is delineated in [21]. Implicit time integration method based on Newton iterations was used for solving kinetic equations system (1)–(3) simultaneously with energy Eq. (4).

Rectangular homogeneous mesh was used for the problem discretization with spatial step $\Delta x = 0.05$ mm. The spatial step was considered enough fine as far as double reduction of spatial step resulted in not more than 2% variation of normal laminar flame velocity in all range of equivalence ratios for accepted mechanism of chemical kinetics.

Combustion ignition is simulated by setting a heat release spot at the stoicheometric line at some fixed distance from the entrance cross-section. At the initial time instant gas has temperature $T_0 = 300$ K. Heat release is switched off after burning started.

4. Results and discussion

The stationary solution being obtained for the model combustion system let one determine effective TF velocity which is equal to velocity of incoming gas $S_f = -u_0$. Local gas velocity thus determines flame propagation speed relatively to given reference point. Typical stationary solution for TF is presented in the Fig. 5. To determine local flame velocity $S_{loc} = -u_{\mathbf{R}}$ in vicinity of flame leading edge, a corresponding reference point **R** should be uniquely defined. We determined reference point by using the fact that mixing parameters χ and μ are monotonous functions of the y coordinate in the case of non-reacting flow. They have extremum in vicinity of the combustion front (coordinate y_{max}) Fig. 6. Physically the extremum corresponds to coordinate where concentration field perturbation caused by combustion takes place. Crossing of the stoichiometric line and y_{max} coordinate line gives one possible reference point **R** for local front velocity determination, Fig. 5. The value of mixing degree parameter in the extremum point χ_{max}. and fuel gradient parameter in the **R** point μ_{max} were used as characteristic values to determine dependences $S_{loc}(\chi)$, $S_{loc}(\mu)$ and $S_f(\chi)$, $S_f(\mu)$ which are of primary interest in this investigation.

A set of runs with different initial mixing degree χ_0 was performed. TF velocity dependence on mixing degree in vicinity of the front was determined, Fig. 7. Flame velocity was normalized by normal laminar flame velocity S_l. The graphs demonstrate that TF propagation speed may considerably exceed normal laminar flame velocity. The function $S_f/S_l = f(\chi)$ has rounded convex

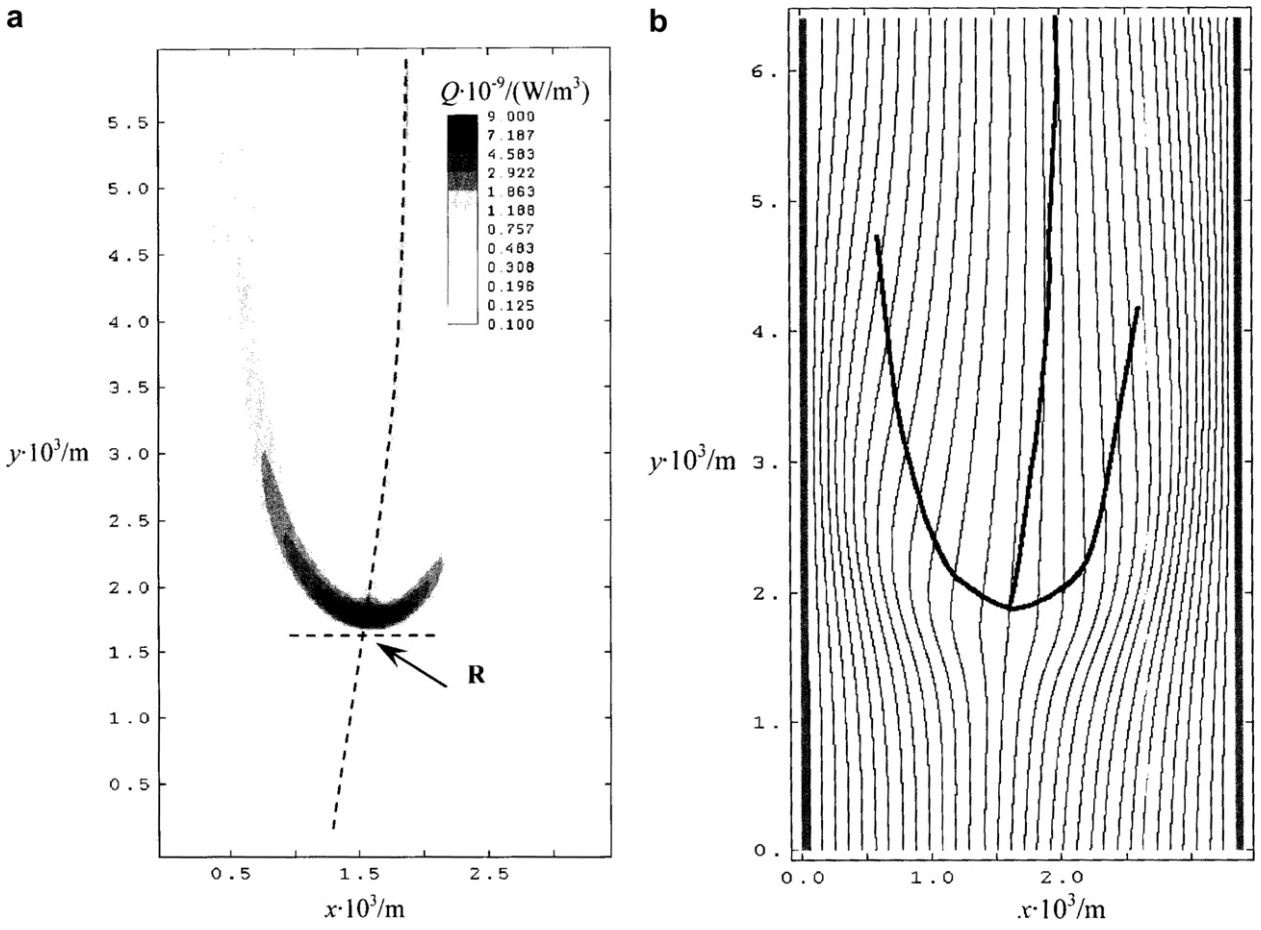

Fig. 5. Heat release field – (a) and flow lines – (b) in stationary triple flame. Mixing at the entrance cross-section $\chi_0 = 0.5$, $d = 3.2$ mm, $L = 6.4$ mm. Dot line – stoicheometric line, dashed line – y_{max} coordinate. **R** – reference point for local flame velocity evaluation.

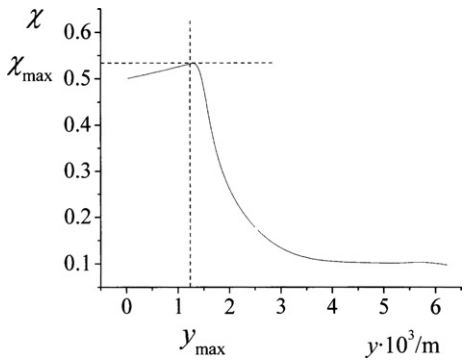

Fig. 6. Mixing degree χ dependence on length along the channel $\chi(y)$. Initial mixing $\chi_0 = 0.5$, $d = 3.2$ mm, $L = 6.4$ mm.

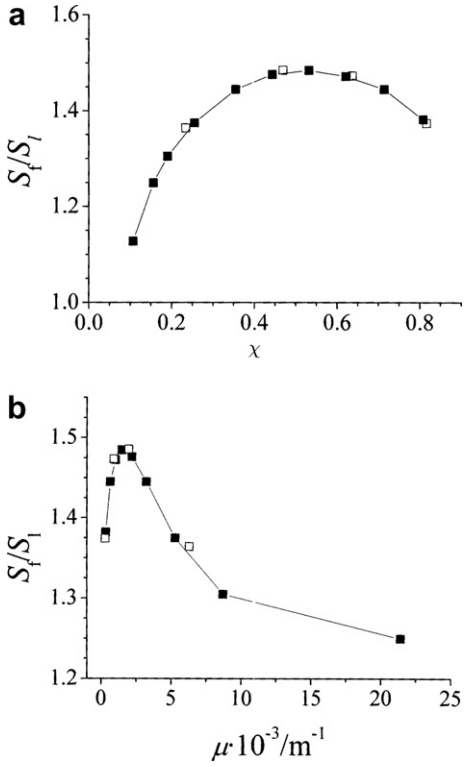

Fig. 7. Dimensionless flame velocity dependence on dimensionless mixing parameters χ – (a), gradient of concentration logarithm μ – (b), $d = 3.2$ mm. ■ – correspond to $L = 6.4$ mm, $y_f = 1.6$ mm; □ – $L = 9.6$ mm, $y_f = 3.2$ mm.

shape with maximum near $\chi = 0.5$ for channel width $d = 3.2$ mm.

The distance of flame stabilization y_f and simulation domain length L may influence TF parameters as far as hydrodynamic field generated by flame (Fig. 5b) may interact with walls and entrance cross-section velocity field. To estimate influence of the distance of flame stabilization on flame velocity a set of numerical experiments was run with increased length of the simulation domain L and flame stabilization length y_f. The data calculated with $L = 9.6$ mm and $y_f = 3.2$ mm parameters are presented on the Fig. 7 with empty boxes and practically coincide with data calculated with $L = 6.4$ mm and $y_f = 1.6$ mm. This confirms that stabilization distance $y_f = 1.6$ mm is enough for adequate simulation of flow field for the given parameters of the system.

The width of the channel is another parameter which can considerably influence TF velocity. Calculations of the flame velocity performed, for several channel widths ($d = 3.3,\ 6.6,\ 9.9$ mm), show that channel width growth leads to monotonous growth of the flame velocity. For fixed μ ($\mu = 1000\ \mathrm{m}^{-1}$) flame velocity grows monotonously with the tendency to saturation, Fig. 8.

The data presented on Fig. 8 may be approximated by exponential function:

$$S_f/S_l = 2.17\left[1 - \exp\left(\frac{d/l_f}{14.8}\right)\right], \tag{7}$$

with accuracy better than 1% (mean squares minimization was used). This gives quantitative estimation of TF maximum velocity: $S_f \approx 2.2 S_l$ for $d \gg l_f$.

Characteristic width of the channel d_{sat} when influence of the walls is negligible and TF velocity is close to maximum depends on mixing degree. Exponential approximation (7) may be utilized for quantitative estimation of this parameter by definition $(d_{sat}/l_f)/14.8 = 3$ or other similar definition. Basing on numerical simulation the following relationship for d_{sat} can be recommended: $d_{sat} \approx 100 l_f \chi$.

The same simulations were performed for axis-symmetric system for different radii of the channel. Fuel was fed in the center and air in the peripheral part of cross-section, Fig. 1.

Flame velocity dependence on the radius of the channel remains the same for axis-symmetrical system, Fig. 9. Tendency to saturation is observed. The following exponential approximations for the data presented in the Fig. 9, were obtained by mean square root method:

$$S_f/S_l = 2.13\{1 - \exp[(r/l_f)/18.3]\}. \tag{8}$$

The local propagation velocity of TF was evaluated for the reference point **R** in vicinity of the flame leading edge, Fig. 10. Calculations show that dimensionless local flame

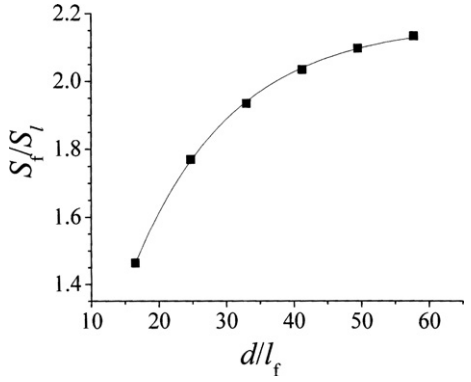

Fig. 8. Dimensionless flame velocity at different channel width ($\mu = 1000\ \mathrm{m}^{-1}$). Solid line – approximation (7).

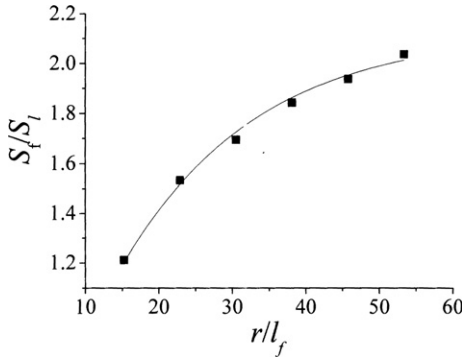

Fig. 9. Dimensionless flame velocity dependence on dimensionless radius of the system ($\mu = 1000\ \mathrm{m}^{-1}$). Solid line – approximation (8).

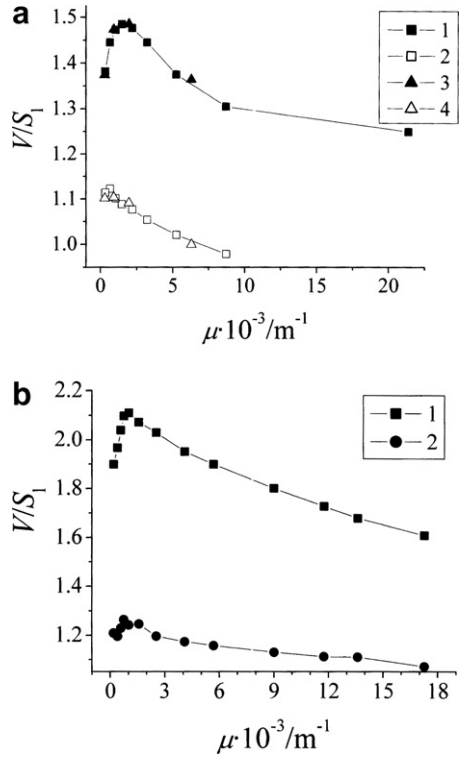

Fig. 10. Flame velocity and local gas velocity before front as a function of mixing parameter μ. (a) 1 – S_f $L = 6.4$ mm, $y_f = 1.6$ mm; 2 – S_f $L - 9.6$ mm, $y_f = 3.2$ mm; 3 – S_{loc} $L = 6.4$ mm, $y_f = 1.6$ mm; 4 – S_{loc} $L = 9.6$ mm, $y_f = 3{,}2$ mm; (b) 1 – S_f $L - 6.4$ mm, $y_f = 1.6$ mm; 2 – S_{loc} $L = 6.4$ mm, $y_f = 1.6$ mm.

velocity S_{loc}/S_l, is close to unity and considerably lower than flame velocity S_f/S_l. Similarity of the shape of the curves $S_f(\mu)$ and $S_{loc}(\mu)$ supposes that streamlines divergence may also affect local velocity S_{loc} although to less extend than S_f, Fig. 10. Relatively small local velocity confirms idea that effective flame velocity doesn't determined by high local speed of the flame edge, but by the hydrodynamic reorganization of the flow field at relatively high distances around flame front.

Series of calculations were performed for maximal channel width and for different concentration gradients. Dependence of the flame velocity on the fuel logarithm gradient for the plain ($d = 9.6$ mm) and axis-symmetrical ($r = 9.6$ mm) channels is presented on the Fig. 11. They have been approximated according following formulas:

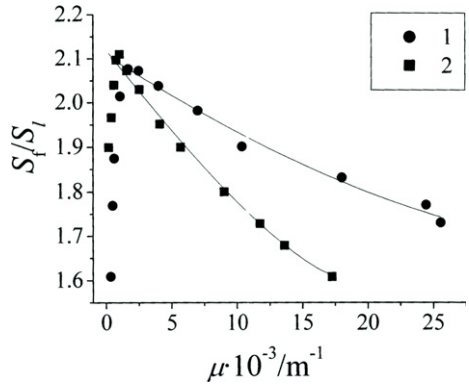

Fig. 11. Dimensionless flame velocity dependence on μ. 1 – plain channel, $d = 3.2$ mm, 2 – axis-symmetrical channel, $r = 3.2$ mm.

$$\frac{S_f}{S_l} = 0.427\left(1 - \frac{\mu}{3.77\cdot10^5}\right)^{1.7} + 1.68,$$

for plain channel,

$$\frac{S_f}{S_l} = 0.506\left(1 - \frac{\mu}{1.73\cdot10^4}\right)^{1.3} + 1.61,$$

for axis-symmetrical channel.

Asymptotic flame front velocities for $\mu = 0$ are close to but less then $\sqrt{\frac{\rho_u}{\rho_{b,st}}}$. For plain channel $\frac{S_f}{S_l} = 2.11$ for axis-symmetrical channel $\frac{S_f}{S_l} = 2.12$ and $\sqrt{\frac{\rho_u}{\rho_{b,st}}} = 2.74$.

5. Conclusions

Velocity of triple flames propagation in plain and axis-symmetrical channel is evaluated numerically. It is shown that velocity of triple flame depends on fuel-oxidizer mixing degree, channel width and symmetry and considerably exceeds normal laminar flame velocity. Flame velocity dependence on concentration logarithm gradients and mixing degree exhibit non-monotonous behavior with maximum. The maximum velocity of the triple flames in plain and axis-symmetrical systems are close and $S_f \approx 2.1 S_l$. The values of the methane concentration logarithm gradients corresponding to the maximum velocity are: $\mu \approx 1000\ \mathrm{m}^{-1}$ for plain and $\mu \approx 2000\ \mathrm{m}^{-1}$ for axis-symmetrical system.

The main mechanism of flame propagation with velocity higher then laminar flame one is gas flow field redirection in front of flame base. At the same time local velocity of the flame front header is relatively close to the normal laminar flame velocity S_l.

Flame velocity increases with the width (or radius) of the channel and comes to saturation at the width estimated as $d_{sat} \sim 100 l_f \chi$.

Acknowledgement

This work was supported by Program of cooperation between CNRS and Academy of Sciences of Belarus for 2005–2006.

References

[1] H. Phillips, in: 10th International Symposium on Combustion, Cambridge, 1965, p. 1277.
[2] J. Buckmaster, Prog. Energy Combust. Sci. 28 (2002) 435–475.
[3] S.H. Chung, Stabilization, propagation and instability of tribrachial triple flames, Proc. Combust. Inst. (2006), doi:10.1016/j.proci.2006.08.117.
[4] S. Ghoshal, L. Vervich, Stability diagram for lift-off and blowout of a round jet laminar diffusion flame, Combus. Flame 124 (4) (2001) 646–655.
[5] A. Upatnieks, J.F. Driscoll, C.C. Rasmussen, S.L. Ceccio, Liftoff of turbulent jet flames – assessment of edge flame and other concepts using cinema-PIV, Combust. Flame 138 (3) (2004) 259–272.
[6] J.W. Dold, Flame propagation in a non-uniform mixture: analysis of a slowly varying triple flame, Combust. Flame 76 (1989) 71–88.
[7] L.J. Hartley, J.W. Dold, Flame propagation in a nonuniform mixture: analysis of a propagating tropple flame, Combust. Sci. Technol. 80 (1991) 23–46.
[8] G.R. Ruetsch, L. Vervisch, A. Linan, Phys. Fluids A 7 (1995) 1447–1454.
[9] B.J. Lee, S.H. Chung, Stabilization of lifted tribrachial flames in a laminar nonpremixed jet, Combust. Flame 109 (1–2) (1997) 163–172.
[10] T. Echekki, J.H. Chen, Structure and propagation of methanol–air triple flames, Combust. Flame 114 (1–2) (1998) 231–237.
[11] H.G. Im, J.H. Chen, Structure and propagation of triple flames in partially premixed hydrogen–air mixtures, Combust. Flame 119 (1999) 436–454.
[12] H.G. Im, J.H. Chen, Comb. Flame 126 (2001) 1384–1392.
[13] Y.C. Chen, R.W. Bilger, Stabilization mechanisms of lifted laminar flames in axisymmetric jet flows, Combust. Flame 123 (1–2) (2000) 23–45.
[14] R.J. Kee, F.M. Rupley, J.A. Miller, M.E. Coltrin, J.F. Grcar, E. Meeks, H.K. Moffat, A.E. Lutz, G. Dixon-Lewis, M.D. Srnooke, J. Warnatz, G.H. Evans, R.S. Larson, R.E. Mitchell, L.R. Petzold, W.C. Reynolds, M. Caracotsios, W.E. Stewart, P. Glarborg, C. Wang, O. Adigun, W.G. Houf, C.P. Chou, S.F. Miller, P. Ho, D.J. Young, CHEMKIN Release 4.0, Reaction Design, Inc., San Diego, CA, 2004.
[15] M.I. Hassan, K.T. Aung, G.M. Faeth, Combust. Flame 115 (1998) 539–550.
[16] X.J. Gu, M.Z. Haq, M. Lawes, R. Woolley, Combust. Flame 121 (2000) 41–58.
[17] C.M. Vagelopoulos, F.N. Egolfopoulos, C.K. Law, Proc. Combust. Inst. 25 (1994) 1341–1347.
[18] A. Van Maaren, D.S. Thung, L.P.H. De Goey, Combust. Sci. Technol. 96 (1994) 327–344.
[19] C.M. Vagelopoulos, F.N. Egolfopoulos, Proc. Combust. Inst. 27 (1998) 513–519.
[20] K.V. Dobergo, I.M. Kozlov, N.N. Gnezdilov, V.V. Vasiliev, 2DBurner – software package for gas filtration combustion and gas non-steady flames simulation, Preprint I, HMTI Publications, Minsk, 2004.
[21] I.M. Kozlov, A. Ye. Suvorov, V.I. Tyukaev, A numerical study of free convection in a strongly inhomogeneous gas medium, Int. J. Heat Mass Transfer 38 (1995) 2689–2695.